Periodico di Mineralogia (2014), 83, 3, 329-344 DOI: 10.2451/2014PM0018

PERIODICO di MINERALOGIA
established in 1930

An International Journal of
MINERALOGY, CRYSTALLOGRAPHY, GEOCHEMISTRY,
ORE DEPOSITS, PETROLOGY, VOLCANOLOGY
and applied topics on Environment, Archaeometry and Cultural Heritage

Iron Age silicate slags from Val Malenco (Italy): the role of textural and compositional studies in the reconstruction of smelting conditions

Fabio Giacometti[1], Gisella Rebay[1], Maria Pia Riccardi[1], Serena Chiara Tarantino[1], Costanza Cucini Tizzoni[2] and Marco Tizzoni[3]

[1]Dipartimento di Scienze della Terra e dell'Ambiente, Università di Pavia, via Ferrata 1, I-27100 Pavia, Italy.
[2]Metallogenesi s.a.s., Via Pria Forà 4, I- 20127 Milano, Italy.
[3]Dipartimento di Lettere e Filosofia, Università di Bergamo, Via Pignolo 123, I-24121, Bergamo, Italy.
Corresponding Author: *fabio.giacometti@unipv.it*

ABSTRACT

A petrographic study of copper smelting slags from several localities of Val Malenco (Italy) provides a key for unravelling the technologies used in reduction of copper ores during the Iron Age.

Thick "tap type" slags with "rope surface" structures and thin, flat slags, were analysed. All slags are made of olivine (up to 60%), oxides, sulfides, minor interstitial Fe-rich pyroxenes (esseneite and augite) and glass. Olivine is zoned, with Mg-rich cores, Fe-rich inner rims and thin Ca-rich outer rims. Observed mesh textures and the compositions of olivine cores and relic minerals, such as Cr-rich spinel, suggest that the mineralised levels of the Malenco ophiolitic complex were the source of the exploited ore. Ca-rich olivine rims and Ca-rich interstitial phases suggest a Ca-rich material was supposedly added during smelting to lower the melting point of the ore. The material used for this task could have been marbles or calcschists of ophicarbonates outcropping nearby Lanzada. Based on petrological considerations, the smelting conditions were constrained to a furnace in which, for temperatures around 1080-1200 °C, oxygen fugacity was 10^{-13}-10^{-8} atm.

Key words: slags; smelting process; copper; sulfides; archaeometry.

Introduction

The determination of the chemical, mineralogical and textural features of slags (i.e. wastes of smelting processes) gives hints on the ancient smelting techniques even when archaeological records of furnaces and other evidences are missing. Archaeometrical studies of slags can give insights on the types of raw and flux material, on the separation of metal from slag, on temperatures and redox conditions within the furnace and on effectiveness of the reduction process (e.g. Bachmann, 1982; Jarrier et al., 1995; Morelli et al., 1998; Menasse and Mellini, 2002; Sáez et al. 2003; Whiteman and Okafor, 2003; Tumiati et al., 2005; Bourgarit et al., 2008; Chiarantini et al., 2009; Humphris et al., 2009; Krismer et al., 2012). The textural and mineralogical evolution of a slag during cooling is the result of the complexity of the smelting process. Different textures, mineralogies and chemical compositions observable in slags of the same excavation site may, for example, reflect different moments of the smelting process or different location of the slag in the furnace and give insights on the possible addition of flux material. In order to obtain information about the smelting process from the study of slags it is necessary to integrate archeological evidence with petrological study of selected, well defined samples from the excavation site.

A petrographic study of a selection of Iron Age copper smelting slags from Campomoro (Val Malenco, Norhtern Italy) is here introduced, following an approach utilized in the study of ancient artefacts (e.g. Bachmann, 1982; Messiga et al., 2004; Rapp, 2009 and references therein). This work emphasises the role played by microtextural and microchemical investigations in collecting information on materials and technologies utilized in manufacturing processes. The petrographic and chemical in-situ analyses applied to significant archeaologically-constrained samples can help answering some of the long lasting questions regarding the techniques of smelting used in ancient metallurgy.

Archaeological setting

The Iron age was a period of flourishing of copper extraction activities in Val Malenco (Northern Italy) as testified by numerous findings of slag deposits throughout the valley (Casini et al, 1999). Piles of silicate slags resulting from this activity, are widespread in a large area between 1660 and 2200 m above sea level.

Campomoro, one of the sites in Val Malenco, was investigated in an archaeological trench in order to provide dating elements, to ascertain the real extension and thickness of the slag layer and, possibly, to collect information about the technology employed by the ancient smelters. Very few wooden shards were found confirming the radiocarbon dating of the site to the Iron Age. Layers of slags and structures related with the smelting activity were discovered, even though no smelting furnace has been found yet (Cucini Tizzoni et al., 2010).

Geological Setting

A metaophiolitic complex, consisting of ultramafics, ophicarbonates, metabasalts and

Mesozoic metasediments outcrops in Val Malenco. Cu-Fe, Fe-Cu-Zn and Fe-Ni-Co ocean-floor related sulfide mineralizations can be recognised in the different lithologies forming the complex (De Capitani et al., 1981). The Val Malenco metaophiolites underwent polyphasic Alpine metamorphism mainly under greenschists facies conditions. Later thermal metamorphism associated with the intrusion of the Bergel pluton overprints the Alpine metamorphism-related features in the western part of the area (Figure 1; De Capitani et al., 1981; Trommsdorff and Evans, 1977).

Slags were found in Campomoro, close to serpentinite outcrops and less than 5 km far from Fe-Ni-Cu sulfides mineralizations (Figure 1). According to Burkhard (1989) ore minerals associated with serpentinites in Val Malenco are magnetite, Cr-spinel, chalcopyrite, pyrrhotite, pentlandite, sphalerite, cubanite, bornite, covellite, cobaltite and mackinawite.

Ultramafites at Val Malenco consist of olivine-antigoritic serpentinites derived from harzburgites and lherzolites. The typical paragenesis consists of antigorite, diopside, olivine and magnetite (De Capitani et al., 1981, and references therein). Serpentinites affected by contact metamorphism are richer in olivine and, depending on the

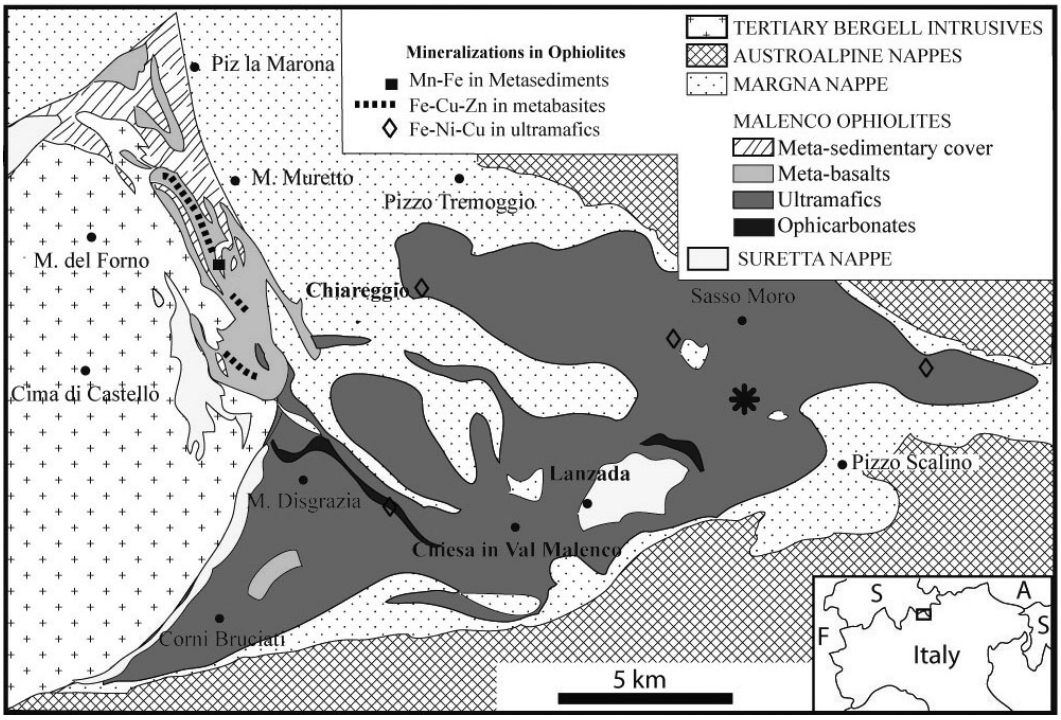

Figure 1. Structural map of the Val Malenco metaophiolitic complex and its mineralization (from De Capitani et al., 1981). Asterisk shows sample location at Campomoro.

metamorphic grade, contain tremolite, talc, anthophyllite, magnesiocummingtonite and enstatite (Trommsdorff and Evans, 1972).

Analytical method

Thin sections of slags from Campomoro (Val Malenco) have been investigated by means of a transmitted/reflected light petrographic microscope and then a further selection was analysed using a scanning electron microscope (SEM) to determine their mineralogies and microstructures.

Spot chemical analyses of the most representative phases related to specific micro-textures were performed at Università degli Studi di Pavia with a JEOL IXA 840A electron microprobe equipped with three wavelength-dispersive spectrometers (TAP, PET and LIF analysing crystals) and one Si(Li) energy dispersive spectrometer (EDS, Be window). The accelerating voltage was 20 kV, the beam current 20 μA, and the spot diameter about 5 micron. Data collected by WDS have been processed with the TASK correction program. Natural minerals (amphibole, omphacite, diopside, ilmenite and chromite) were used as standards to minimise matrix effects. Estimated precision is about 3% for major- and 10% for minor-elements respectively. Estimates of ferric and ferrous iron contents were based on charge balance calculations.

Microtextures

Two typologies of slags with different morphologies and textures were investigated. “Thin slags”, a few millimetres thick, have flat surfaces and well developed flow textures. “Thick slags”, up to some centimetres thick, are variably porous and have rope surfaces. Thin slags are texturally homogeneous being made of skeletal and chain olivine (~50%), dendritic wustite (~37%), interstitial glass (~10%) and minor clinopyroxene, spinel and sulfide globules (Figure 2A-C). The surface and the first 0.5 mm are slightly altered, with widespread oxidation (Figure 2A). Olivine is slightly zoned with Fe content increasing towards the rims. Skeletal olivine crystals include rounded wustite drops and, locally, sulfides (Figure 2C). Wustite blobs and dendrites are aligned along preferential directions corresponding to crystallographic orientations (Figure 2B).

Thick slags (Figure 3A-F) are mainly made of euhedral, hopper and, locally, chain olivine (40 - 60%), spinel (5 - 20%), glass (15 - 30%), clinopyroxene (5 - 15%), sulfide and metals globules (3 - 7%), wustite (1 - 3%) and blisters, in variable proportions (0 - 30%). Olivines are scattered in a fine-grained matrix of glass and acicular pyroxene and, locally, are surrounded by a silicate phase, generally a pyroxene (Figure 3C and D).

The different shapes of olivine can occur in each sample, but euhedral polygonal olivines are the most widespread in thick slags. Olivines are optically and compositionally zoned, with, locally irregular shaped, forsteritic cores, fayalitic inner rims and Ca-rich outer rims. Locally, olivine crystals are rimmed by clinopyroxene (Figure 3D). Wustite and spinel

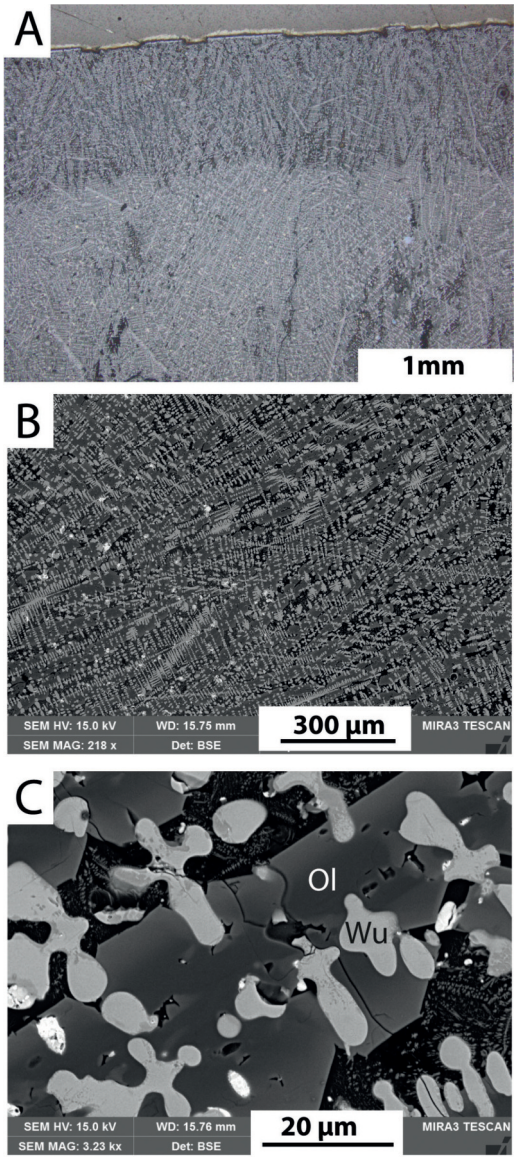

Figure 2. Microtextural features of thin slags at different scales. A) reflected light microscope photomicrograph of a thin slag; B) BSE image of skeletal olivines and dendritic wustites are the most abundant phases in thin slags. C) detail of a skeletal olivine and dendritic wustite in a glass + pyroxene matrix; thin slag.

occur around the fayalitic inner rims (Figure 3D), but are not included in the cores of olivines, except for one single sample, in which spinel is included in forsterite and fayalite. Spinel and wustite are generally intergrown and in textural equilibrium. Only locally wustite rims spinel (Figure 5C) and viceversa, therefore indicating that the two phases mainly crystallized simultaneously. Spinel is locally zoned with Cr rich cores and Fe-rich rims.

Textures are heterogeneous even at the sample scale. Textural relics of the original rocks are observed in different portions of the slags (Figure 3), but relic minerals themselves are scarce or absent in some of the samples.

Relics of mesh textures seem to occur (Figure 3E): wustite, spinel and minor olivine linear aggregates form a net surrounding polygonal shaped olivine and spinel aggregates resembling mesh textures found in serpentinites.

Textural clinopyroxene relics can be recognised in prismatic aggregates, aligned along the former cleavage, which are made of small olivines, subordinate sulfide globules and, locally, spinels (Figure 3B and F).

Locally fine-grained wustite- and spinel-rich enclaves are isolated within the olivine-rich slag (Figure 3E). Sometimes these enclaves also contain sulfides.

Circular blisters (sub-millimetre to 1 millimetre, up to 5% vol) are widespread only in some of the thick slags (Figure 3A) with the lowest spinel and the highest pyroxene and glass contents.

Opaque minerals and metallic phases were identified under reflected light microscopy and

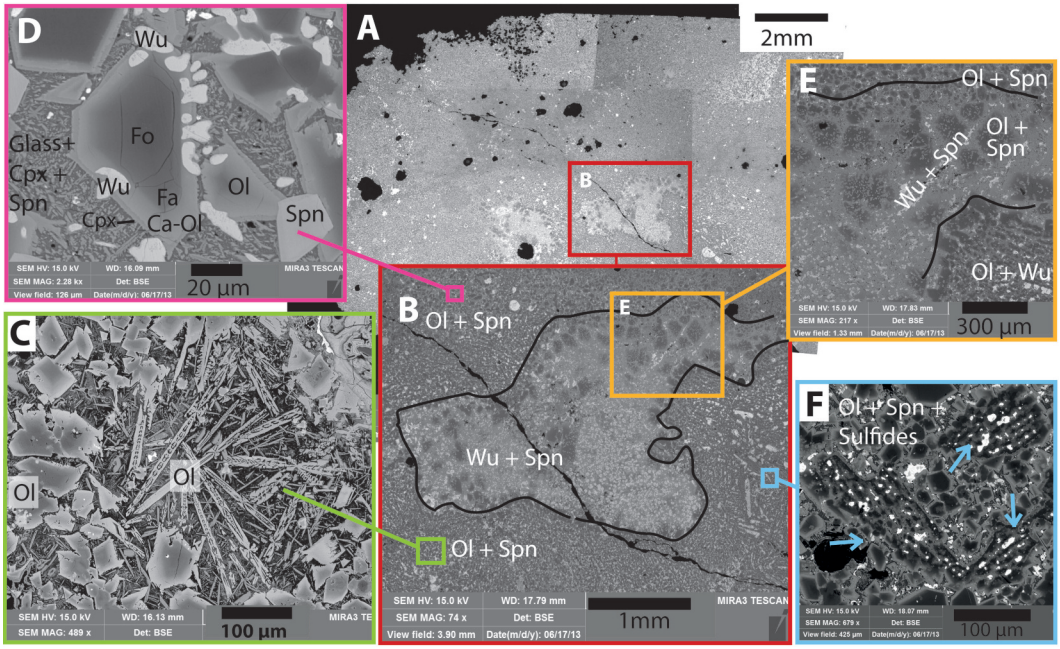

Figure 3. BSE images of textural features of thick slags. A) photomicrograph of a thick slag showing textural heterogeneity. B) Heterogeneities in a thick slag where a wustite- and spinel-rich enclave is surrounded by olivine and spinel rich aggregates. C) Euhedral zoned olivines and chain-olivine occur within few microns in a thick-slag sample. D) Zoned olivine with a forsteritic core and fayalitic to Ca-olivine rims, surrounded by clinopyroxene. Wustite grows with Ca-rich olivine and clynopyroxene growth which are later than that of fayalitic inner rims. E) Detail of B showing relic mesh-like textures. F) Detail of B showing a wustite + spinel enriched zone, on the left, and an olivine + wustite zone on the right. Blue arrows indicate textural relics of former pyroxenes.

EDS and WDS analyses were performed. No relics of primary ore-minerals seem to be preserved.

Pyrometallurgical sulfides are found in 1 to 200 µm sized prills in both thick and thin slags (Figure 4A-B) and in interstices among new-grown olivines in thick slags (Figure 4C). They mainly consist of Cu-Fe sulfides (optically chalcopyrite with exsolution flames of bornite and idaite and bornite-idaite with exsolution of chalcopyrite), pyrrhotite, (locally Co-rich) pentlandite and pyrite, whereas wustite is the main oxide.

Irregular to cubic shaped Fe-Ni ± Cu ± Co alloy scraps are associated with sulfides. The alloy is never in direct contact with the pyrometallurgical Cu-Fe sulfides: pyrrhotite and (Co-rich) pentlandite coronae (with minor pyrite) rim the alloy in the drops. Cu-Ni veins cross the prills and locally Cu-Fe sulfides are replaced by covellite along fractures (Figures. 4A and B). Cu-Ni veins often connect the

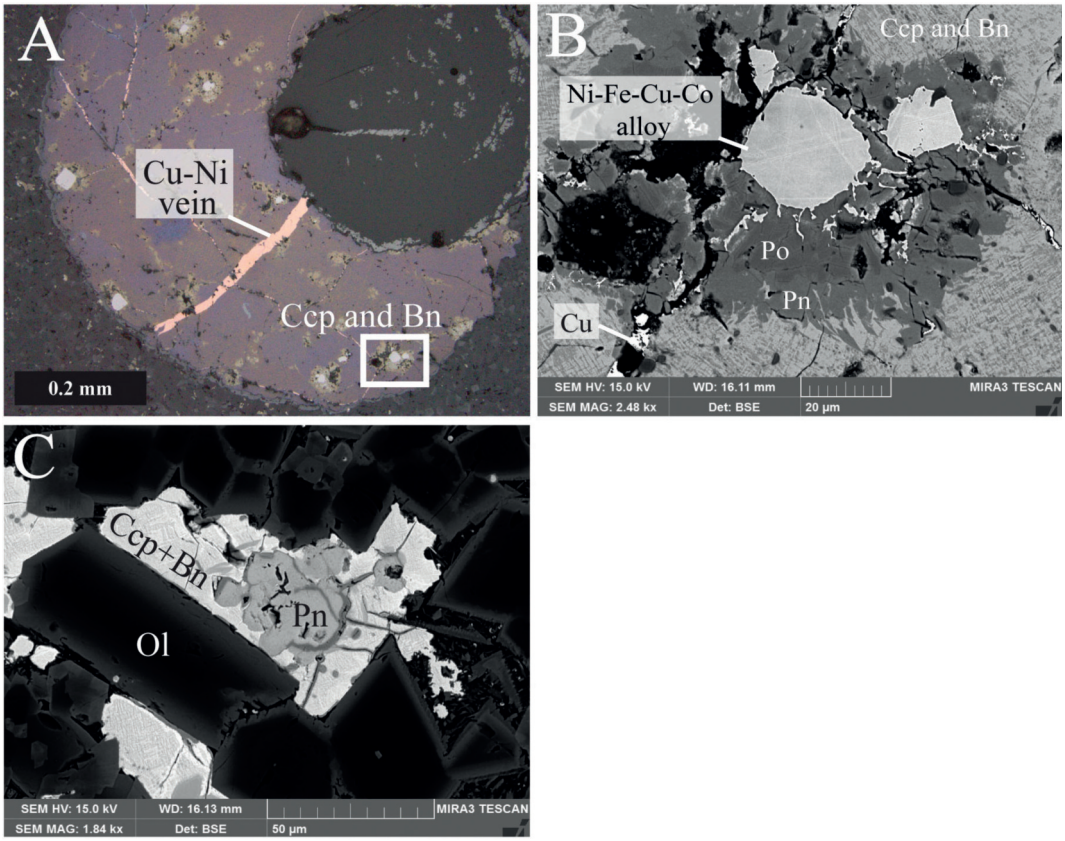

Figure 4. Textural features of sulfides and alloys in thick slags. A) Reflected light microscope image of a sulfides drop with main Cu-Fe sulfides (chalcopyrite, bornite and idaite), metallic copper and metallic alloys. B) BSE detail of the area in the white frame of the previous image. Ni-Fe-Cu-Co alloy scraps rimmed by pyrrhotite and pentlandite coronas are scattered in the sulfide drop. Flame exsolution lamellae of chalcopyrite occur in the bornite and idaite aggregate. C) Pentlandite scrap in the Cu-Fe sulfides (bornite with chalcopyrite exsolutions) intergranular aggregate among euhedral olivines.

Fe-Ni ± Cu ± Co alloy with the rim of prills. Prills are always rimmed by wustite.

Mineral Chemistry

The compositions of silicates, silicate glass, oxides and sulfides are reported in Tables 1, 2, 3, 4, 5 and 6 and 7.

Olivines are slightly zoned in thin slags with Mg-richer cores (Mg up to 1.02 a.p.f.u.) and almost pure fayalitic rims (Fe up to 1.73 a.p.f.u; Figures 5A and B).

Zoning in olivines is more pronounced in thick slags. The large and complex, euhedral olivine crystals have a strong compositional zoning with Mg-rich cores (Mg around 1.65 a.p.f.u., with few

higher values up to 1.91 a.p.f.u.) rimmed by Fe-rich inner-rims (Fe up to 0.95 a.p.f.u.) and Ca-Fe-rich (respectively up to 0.49 and 1.20 a.p.f.u.) thin (~15 μm) external-rims (Figures 5A and B; see Table 1).

Locally olivine displays different textures and less pronounced zoning in thick slags: skeletal olivine has Ca-poorer external rims (with maximum Ca content up to 0.15 a.p.f.u.), and the smallest crystals are almost not zoned (Fe-Mg substitution generally limited to 0.1-0.6 a.p.f.u. from core to rim and no Ca enrichment; Table 2).

Spinels are represented both by Cr-rich hercynite and Fe-rich spinels (Table 3). Zoned spinels have been observed: in Figures 5C and D, a zoned spinel is characterised by a decreasing of Cr from 0.72 to 0.09 a.p.f.u. and Mg (0.41 to 0.23 a.p.f.u.) and increasing Al (0.81 to 1.03 a.p.f.u.) and Fe (Fe^{2+} from 0.59 to 0.77 a.p.f.u.; Fe^{3+} 0.44 to 0.81 a.p.f.u.) from core to rim (Figures 5C and D and Figure 6). Similar variations are observed in spinels among the small euhedral olivines (Table 3).

Interstitial phases among olivine crystals are Fe-rich clinopyroxene and glass (Table 4). The clinopyroxene has peculiar compositions due to high Ca, Al and Fe^{3+} contents (the last being estimated from charge balance). Its composition is intermediate between augite and esseneite end-members. Small acicular crystals are dispersed in

Table 1. Composition of a large zoned olivine crystal.

	LARGER EUHEDRAL OLIVINE								
	core →								rim
SiO_2	39.57	39.25	39.56	38.78	38.87	35.30	36.86	32.63	31.99
TiO_2	0.07	0.09	0.07	0.11	0.13	0.25	0.17	0.38	0.33
Al_2O_3	0.12	0.14	0.09	0.11	0.14	0.08	0.10	0.10	0.03
Cr_2O_3	0.00	0.00	0.00	0.00	0.00	0.00	0.00	0.00	0.08
FeO	15.98	17.94	16.07	20.06	19.34	40.73	29.49	50.63	47.86
MnO	0.14	0.15	0.16	0.17	0.17	0.35	0.25	0.49	0.42
MgO	43.74	42.06	43.61	40.30	40.82	23.98	31.33	13.43	5.35
CaO	0.39	0.36	0.40	0.54	0.52	1.29	1.81	2.37	14.87
Tot wt.%	100.01	99.99	99.96	100.07	99.99	101.98	100.01	100.03	100.93
n. ox.	4.00	4.00	4.00	4.00	4.00	4.00	4.00	4.00	4.00
Si	1.00	1.00	1.00	1.00	1.00	0.99	1.00	0.99	0.99
Ti	0.00	0.00	0.00	0.00	0.00	0.01	0.00	0.01	0.01
Al	0.00	0.00	0.00	0.00	0.00	0.00	0.00	0.00	0.00
Cr	0.00	0.00	0.00	0.00	0.00	0.00	0.00	0.00	0.00
Fe^{2+}	0.34	0.38	0.34	0.43	0.41	0.95	0.66	1.29	1.24
Mn	0.00	0.00	0.00	0.00	0.00	0.01	0.01	0.01	0.01
Mg	1.65	1.60	1.65	1.55	1.57	1.01	1.27	0.61	0.25
Ca	0.01	0.01	0.01	0.01	0.01	0.04	0.05	0.08	0.49
Sum cat	3.00	3.00	3.00	3.00	3.00	3.00	3.00	3.00	3.00

Table 2. Composition of small euhedral and skeletal olivine crystals.

	SMALL EUHEDRAL OLIVINE				SKELETAL OLIVINE		
	core	rim	core	rim	core	⟶	rim
SiO_2	37.71	38.39	41.76	37.95	38.14	35.64	32.53
TiO2	0.02	0.04	0.00	0.03	0.03	0.04	0.14
Al_2O_3	0.08	0.02	0.15	0.12	0.15	0.17	0.37
Cr_2O_3	0.03	0.13	0.00	0.20	0.12	0.15	0.17
FeO	25.92	22.15	4.67	23.24	23.32	36.12	50.18
MnO	0.19	0.17	0.15	0.15	0.15	0.19	0.28
MgO	35.77	38.39	53.26	37.53	37.29	26.16	11.45
CaO	0.27	0.69	0.00	0.81	0.81	1.55	4.91
Tot wt.%	99.99	99.98	99.99	100.03	100.01	100.02	100.03
n. ox.	4.00	4.00	4.00	4.00	4.00	4.00	4.00
Si	1.00	1.00	1.00	0.99	1.00	1.00	1.00
Ti	0.00	0.00	0.00	0.00	0.00	0.00	0.00
Al	0.00	0.00	0.00	0.00	0.00	0.01	0.01
Cr	0.00	0.00	0.00	0.00	0.00	0.00	0.00
Fe^{2+}	0.57	0.48	0.09	0.51	0.51	0.84	1.28
Mn	0.00	0.00	0.00	0.00	0.00	0.00	0.01
Mg	1.42	1.50	1.91	1.47	1.46	1.10	0.53
Ca	0.01	0.02	0.00	0.02	0.02	0.05	0.16
Sum cat	3.00	3.00	3.00	3.00	3.00	3.00	2.99

Table 3. Spinel composition.

	ZONED SPINEL		SPINEL IN OLIVINE		
	core	rim			
TiO_2	1.04	2.48	1.17	1.33	0.88
Al_2O_3	21.47	27.21	22.77	20.75	26.51
Cr_2O_3	28.50	3.36	25.45	15.18	11.45
FeO	40.20	61.95	42.81	55.8	51.34
MnO	0.12	0.18	0.12	0.13	0.13
MgO	8.65	4.81	7.69	6.79	9.66
CaO	0.01	0.01	0.00	0.00	0.00
Tot wt.%	99.99	99.99	100.01	99.98	99.97
n. ox	4.00	4.00	4.00	4.00	4.00
Ti	0.03	0.06	0.03	0.03	0.02
Al	0.81	1.03	0.86	0.80	0.98
Cr	0.72	0.09	0.64	0.39	0.28
Fe^{3+}	0.44	0.81	0.47	0.78	0.72
Fe^{2+}	0.59	0.77	0.63	0.66	0.55
Mn	0.00	0.00	0.00	0.00	0.00
Mg	0.41	0.23	0.37	0.33	0.45
Ca	0.00	0.00	0.00	0.00	0.00
Sum cat	3.00	2.98	2.99	2.99	2.99

Table 4. Clinopyroxene analyses (cpx).

	CPX	CPX	CPX	CPX
SiO_2	38.30	38.41	49.14	46.29
TiO_2	1.86	1.76	0.71	0.87
Al_2O_3	12.75	12.07	15.44	15.54
Cr_2O_3	0.01	0.03	0.14	0.09
FeO	20.70	20.93	16.75	18.94
MnO	0.09	0.15	0.19	0.24
MgO	3.97	4.01	3.10	2.29
CaO	22.18	21.81	11.09	12.21
Na_2O	0.21	0.18	0.46	0.36
K_2O	0.00	0.04	0.60	0.65
Tot wt.%	100.07	99.39	97.62	97.48
n.° ox	6	6	6	6
Si	1.51	1.53	1.86	1.79
Ti	0.06	0.05	0.02	0.03
Al	0.59	0.57	0.69	0.71
Cr	0.00	0.00	0.00	0.00
Fe^{3+}	0.28	0.30	0.00	0.00
Fe^{2+}	0.37	0.36	0.53	0.61
Mn	0.00	0.01	0.01	0.01
Mg	0.23	0.24	0.18	0.13
Ca	0.94	0.93	0.45	0.51
Na	0.02	0.01	0.03	0.03
K	0.00	0.00	0.03	0.03
Sum cat	4.00	4.00	3.80	3.85

glass (Figure 3D) but, because they are smaller than the electron beam size, their composition, which is similar to that of bigger crystals, was only estimated qualitatively.

Glass is heterogeneous at the sample scale (Table 5). Furthermore compositional differences are apparent comparing thick and thin slags. In thin slags, glass has the lowest SiO_2, Al_2O_3 and CaO and the highest FeO contents (Table 5). In both thick and thin slags the variable contents of the oxides listed above reflect the incomplete mixing of the melt during the smelting process (Table 5).

Cu/Fe ratios (calculated on the basis of their wt.% abundance) around 0.47 are observed in pyrometallurgical chalcopyrite. Other Cu-Fe phases are optically similar to bornite and idaite but are richer in Fe than stechiometric minerals ($15 < Fe < 21$ wt.%): according to WDS micro-analyses many of them would have the formula Cu_3FeS_3.

Pentlandite with up to 26 wt.% in Ni is observed. Fe-Ni ± Cu ± Co alloys with up to 61 wt.% in Ni and Cu-Ni veins with up to 86 wt.% in Cu were observed. Co is present in low concentrations and therefore it was only observed quantitatively in SEM-EDS.

Table 5. Composition of glass in thick and thin slags.

	GLASS IN THICK SLAGS			GLASS IN THIN SLAGS		
SiO_2	51.87	45.23	42.33	41.86	38.93	37.35
TiO_2	0.00	0.51	0.00	0.00	0.00	0.37
Al_2O_3	14.86	16.37	18.63	14.53	7.69	14.86
Cr_2O_3	0.00	0.00	0.00	0.00	0.00	0.04
FeO	12.08	19.16	16.38	24.08	39.57	28.31
MnO	0.00	0.00	0.00	0.00	0.00	0.13
MgO	1.02	0.00	1.26	0.00	0.00	0.1
CaO	11.73	13.49	13.19	8.00	4.00	14.2
Na_2O	3.17	3.01	4.17	4.00	3.93	2.4
K_2O	3.52	1.33	2.41	4.00	2.48	3.13
Tot wt.%	98.25	99.10	98.37	96.47	96.6	100.89

Discussion and conclusions

Silicate slags are the result of the separation, during the reduction process of a portion rich in silicates (the slag, result of the crystallisation of melted gangue + melting additive + a certain percentage of metal) from the portion enriched in metal (metal + impurities).

Based on their morphological, textural and mineralogical features (e.g. Bachmann, 1982), thin slags are here interpreted as tap slags representing the silicate melt which was removed from the furnaces during smelting. Thick slags correspond to furnace slags which remained into the kiln during the process.

As the separation process in Iron Age furnaces was not totally efficent, "primary mineral" relics and metallic phases produced during the reduction process (matte) are present in the slags.

Olivine cores have a forsteritic composition, with Mg contents around 1.65 apfu, and spinel have Cr-rich cores with Cr contents up to 0.72. All these values are similar to those observed in peridotites from different ophiolitic sequences (Piccardo et al., 1988). It is thus reasonable to assume that the ore reduced in Val Malenco came from the mineralised levels rich in Fe-Ni-Cu sulfides and Fe-oxides of the Malenco ophiolitic complex which outcrop close to the area in which the slags are concentrated. Microstructures depicted in Figure 3E represent textural relics of the original enclosing rocks (i.e. serpentinites) and Cr-rich spinels could represent a relic phase of ultramafic rocks. Also Mg-rich olivine cores probably correspond to remains of the original paragenesis: pyrometallurgical olivines with MgO around 43 wt.% would indicate smelting temperatures over 1500 °C which are unlikely for Iron age furnaces (e.g. Bourgarit et al., 2008). However, flux addition could lower the liquidus temperature of the system, therefore a pyrometallurgical origin of Mg-rich olivines cannot be completely discounted a priori. Alternatively Mg-rich olivines could form at temperatures above 400 °C from antigorite—bearing assemblages (cf. Bucher and Grapes, 2011) due to solid state de-hydration reactions in

the smelting furnace, but this option seems to be more unlikely.

Temperatures obtained in the furnace were such as to provoke the almost complete melting of the silicate portion, as shown by the almost complete recrystallization and by the resorbtion textures in the larger Mg-rich olivines. Scheletric textures in olivines testify fast cooling.

Cucini Tizzoni et al. (2010) estimated furnace temperatures during the smelting process, based on the chemical composition of interstitial glass in copper slags from Val Malenco. The authors plotted the composition of interstitial glass of thick and thin slags in the $SiO_2 – Al_2O_3 – CaO$ and $SiO_2 – Al_2O_3 – FeO$ ternary liquidus phase diagrams respectively. The compositions plot close to eutectics at the temperatures of 1080 and 1200 °C, which are interpreted as the minimum possible peak temperatures reached during smelting. Temperatures between 1100 and 1150 °C are inferred plotting the composition of the Cu-Ni veins found in the present work in the Cu – Fe – Ni ternary diagram proposed by Starykh and Sineva (2011), which supports previous estimates.

Compositional variations in olivines, from Mg-rich inner rims, to Fe-rich rims with a thin Ca-rich outermost rim, are compatible with a decrease in temperature (Mg- to Fe-rich) and suggest that during the reduction process a Ca-rich melting additive was employed. In fact the serpentinites and the enclosed mineralizations do not contain enough Ca to allow the formation of such Ca-rich phases (olivine rims, pyroxene and glass) in the modal quantity observed in the slags. It is suggested that the melting additives were marbles and/or ophicarbonates and/or calcschists that outcrop widely nearby Campomoro (Figure 1; Beltrami et al., 1974).

Interpretation of the oscillatory zoning in the minerals is not unequivocal as it could be due to:

1. sudden temperature lowering in the furnace;
2. variations in the chemical potential due to the variation of the oxidation state in the furnace;
3. compositional variations of the system due to the extraction of melt and/or addition of flux.

As all these processes may happen contemporaneously in ancient kilns, due to the repeated recharges of the furnace during the smelting process, the importance of each of them cannot be ascertained without having samples whose location within the furnace is well known

The presence of “matte” in slags is frequently recorded in the literature (e.g. Chiarantini et al., 2009; Krismer et al., 2012; Manasse and Mellini 2002; Tumiati et al., 2005). The low sulfides content in the slags and the presence of Cu-Ni veins and metal alloys prills within the sulfide aggregates indicate that the smelting process was rather efficient at Campomoro. Based on the textural and chemical features of both sulfide prills and interstitial aggregates among olivines, no relics of the original metallic paragenesis occurs: both prills and interstitial aggregates seem to be derived from a sulfide rich melt which was separated from the silicate melt and then was trapped among the olivine (± spinel ± wustite) cristalline frame.

Furthermore the occurrence of metal alloys scraps, veins and prills within the sulfide aggregates indicate that a Cu-Ni-Fe-rich S-free melt could separate from the sulfide-rich melt.

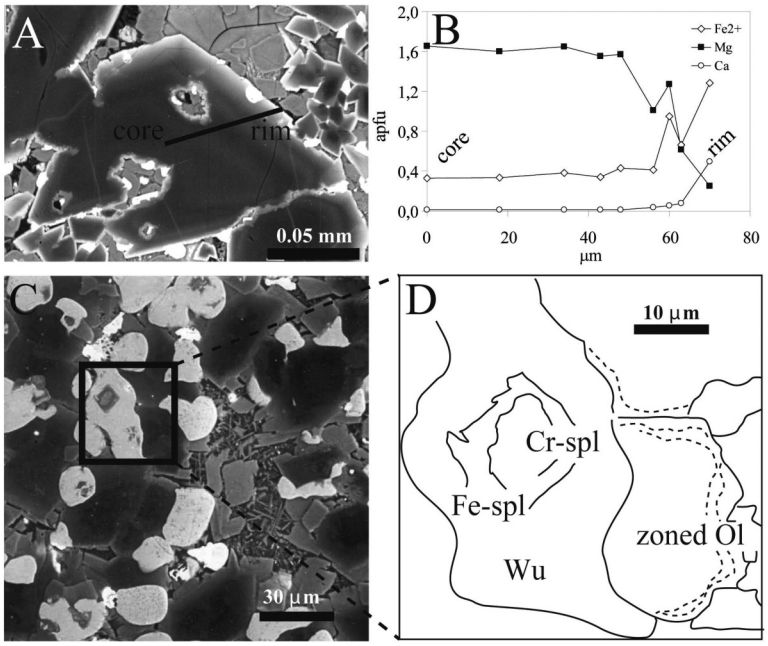

Figure 5. Zoning in olivines and spinels. A) Zoned hopper olivine (BSE image). The white transect corresponds was analyzed with the EPMA. B) The chemical profile of the transect in the previous image showing the variations in Fe^{2+}, Mg and Ca contents of the zoned olivine crystal. C) and D) Schematic representation of zoning in olivine and spinel crystals.

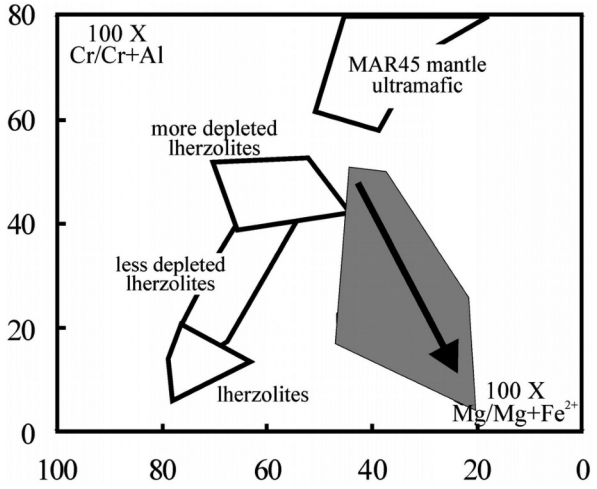

Figure 6. Compositional zoning in spinels compared to mantle spinel compositions.

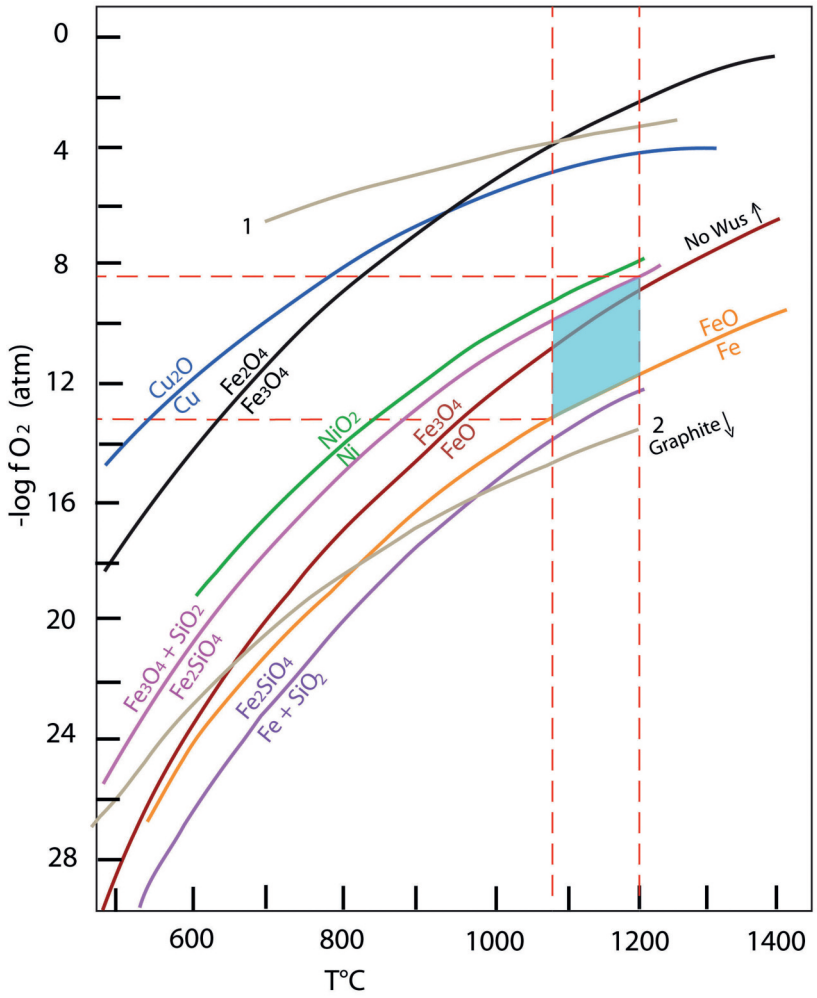

Figure 7. Dependance of –log fO_2 on T for copper smelting (after Chiarantini et al., 2009). Curve 1 represents the CO_2 – (CO + CO_2) limit and curve 2 represents the (CO + CO_2) – graphite limit. The light blue area is defined on the basis of the observed mineralogy and temperature estimates by Cucini Tizzoni et al. (2010).

Cu-Ni veins connecting the alloy scrap with the rim of the sulfide prills probably represent the pathways of metallic Cu removed from the slag. According to Burger et al. (2011 and references therein), a solid state reaction of desulfurization of chalcopyrite can occur at the beginning of the smelting process leaving a residual Cu-Fe sulfide with modified stechiometry: $CuFeS_{2(s)} + (3\text{-}y - z)/2O_{2(g)} \rightarrow Cu_xFe_yS_{z(s)} + (1\text{-}x)\,Cu_{(s)} + (1\text{-}y)\,FeO_{(s)} + (2\text{-}z)\,SO_{2(g)}$

A solid state diffusion of Fe^{2+} and S^{2-} towards the rim of the chalcopyrite aggregates would determine the release of S and the development of a Fe-oxide corona around the aggregate and determine a Cu enrichment to occur within the residual sulfide (e.g Bourgarit et al. 2008; Burger et al., 2011). Textural evidences provided in this work suggest that a similar process is likely to have occurred also in the po + ccp + pn aggregates of the original metallic paragenesis at Campomoro.

The exsolved Fe-Cu sulfides associated with chalcopyrite (optically bornite and idaite, but Fe richer than stechiometric formulas) have lower wt.% Fe/Cu and S/Cu ratios (between 0.26 and 0.43 and between 0.46 and 0.61 respectively) than the Cu-Fe disulfide. Probably these relatively low Fe and S contents are the consequence of the removal of Fe and S from chalcopyrite and their diffusion towards the external surface of the prills where iron forms wustite and S is removed as a gaseous phase (probably SO_2; e.g. Burger et al. 2011). The progressive Fe and S removal would be responsible for the segregation of Fe-Ni ± Cu ± Co alloys within sulfide prills and for the development of metallic veins (Figure 4).

The abundance of wustite and the absence of pure magnetite, can be due to a highly reducing atmosphere in the furnaces (e.g. Burger et al. 2011). However the occurrence of ferric iron in spinels was identified based on charge balance calculations. On this basis, considering the mineralogy of slags, the redox conditions varied in a narrow range, among the iron-wustite and the fayalite-Fe_3O_4+SiO_2 buffers in the –log f O_2 vs T diagram. Temperatures estimated by Cucini Tizzoni et al. (2010) together with the mineralogical composition of slags can be used to approximately estimate the oxygen fugacity within the furnace during the smelting process. f O_2 values between 10^{-13} and 10^{-8} atmospheres are obtained in a –log f O_2 vs T diagram (Figure 7).

The petrographic study of the Val Malenco slags allowed to define the materials utilized during the reduction process. Moreover, the application of a petrologic approach, which combines microstructural analysis, mineralogical and in situ chemical analyses, to artificial rock-like materials, gives hints on the quantification of some of the parameters operating during the smelting process: combined investigations of the silicate portion of the slags and of oxides and sulfides, allowed to deduce temperatures attained in the furnace and to evaluate the oxidation conditions at which the reduction process took place.

REFERENCES

Bachmann H.G. (1982) - The Identification of Slags from Archaeological Sites. University of London, Institute of Archaeology, London, 82 pp.

Beltrami G., Liborio G., Montrasio A. and Mottana A. (1974) - La “finestra” di Lanzada (Val Malenco, Sondrio). *Società Italiana di Mineralogia e Petrologia*, XXX (2), 839-853.

Bourgarit D., Rostan P., Burger E., Carozza L., Mille B. and Artioli G. (2008) - The beginning of copper mass production in the western Alps: the Saint-Véran mining area reconsidered. *Historical Metallurgy*, 42, 1, 1-11.

Burger E., Bourgarit D., Frotté V. and Pilon F., (2011) - Kinetics of iron-copper sulphides oxidation in raltion to protohistoric smelting. *Journal of Thermal Analysis and Calorimetry*, 103, 249-256.

Bucher K. and Grapes R. (2011) - Petrogenesis of Metamorphic Rocks (8th edition). Springer-Verlag, Berlin, Heidelberg, 428 pp.

Burkhard D.J.M. (1989) - Co-Ni-As Sulphides in Serpentinites of Different Metamorphic Grade in the Eastern Central Alps (Switzerland and Italy). *Mineralogy and Petrology*, 41, 65-71.

Casini S., Cucini Tizzoni C., Marziani G., Tizzoni M. and Zahova A. (1999) - Campomoro (Val Malenco-Sondrio): un impianto di riduzione del rame dell'età del Ferro. *Notizie Archeologiche Bergomensi, Civico Museo Archeologico di Bergamo*, 7, pp.179-205

Chiarantini L., Benvenuti M., Costagliola P., Fedi M.E., Guideri S. and Romualdi A. (2009) - Copper production at Barati (Populonia, southern Tuscany) in the early Etruscan period (8th-9th centuries B.C.). *Journal of Archaeological Science*, 36, 1626-1636.

Cucini Tizzoni C., Messiga B., Rebay G. and Riccardi M.P. (2010) - La riduzione del rame in Val Lanterma (Sondrio) nella prima età del Ferro: studio petrografico delle scorie silicatehe. *Notizie Archeologiche Bergomensi*, 18, 215-230.

De Capitani L., Ferrario A. and Montrasio A. (1981) - Metallogeny of the Val Malenco metaophiolitic complex, Central Alps. *Ofioliti*, 6 (1), 87-100.

Humphris J., Martinón-Torres M., Rehen T. and Reid A. (2009) - Variability in single smelting episodes - a pilot study using iron slag from Uganda. *Journal of Arcaeological Science* 36, 359-369.

Jarrier C., Domergue C., Pieraggi B., Ploquin A. and Tollon F. (1995) - Caractérisation minéralogique, géochimique et métallurgique des résidus de réduction directe, d'épuration et de forge du centre sidérurgique romain des Mertys (Aude, France). *Revue d'Archéometrie*, 19, 49-61.

Krismer M., Töchterle U., Goldenberg G., Tropper P. and Vavtar F. (2012) - Mineralogical and petrological investigations of early Bronze Age copper-smelting remains from the Kiechlberg (Tyrol, Austria). *Archaeometry*, doi: 10.1111/j.1475-4752012.00709.x.

Manasse A. and Mellini M. (2002) - Chemical and textural characterization of medieval slags from the Massa Marittima smelting sites (Tuscany, Italy). *Journal of Cultural Heritage*, 3, 187-198.

Messiga B., Riccardi M.P., Rebay G., Basso E. and Lerna S. (2004) - Microtextures recording melting-history of a medieval glass cake. *Journal of Non-Crystalline Solids*, 342, 116-124.

Morelli I., Benvenuti M., Mascaro I. and Tanelli G. (1998) - Studio comparato di antiche scorie ferrifere provenienti da siti archeometallurgici dell'Isola d'Elba e del Chianti fiorentino. Atti della X giornata "Le Scienze della Terra e l'Archeometria", Napoli, 45-48.

Piccardo G.B., Messiga B. and Vannucci R. (1988) - The Zabargad peridotite-pyrossenite association: petrological constraints on its evolution. *Tectonophysics,* 150, 135-162.

Rapp G. (2009) - Archaeomineralogy. Natural Sciences in Archaeology (2nd Ed.). Springer-Verlag, Berlin, 348 pp.

Sáez R., Nocete F., Nieto J.M., Capitán M.A. and Rovira S. (2003) - The extrusive metallurgy of copper from Cazebo Juré, Huelva, Spain: chemical and mineralogicl study of slags dated to the third millenium B.C. *The Canadian Mineralogist*, 41, 627-638.

Starykh R.V. and Sineva S.I (2011) - Study of the Liquidus and Solidus Surfaces of the Quaternary Fe-Ni-Cu-S system: V. Refinement and Addition of the Data on the Ternary Fe-Ni-S and Fe-Ni-Cu Phase Diagrams. *Russian Metallurgy*, 22, 189-194.

Trommsdorff V. and Evans B.W. (1972) - Progressive metamorphism of antigorite schist in the Bergell tonalite aureole (Italy). *American Journal of Science*, 272, 423-437.

Trommsdorff V. and Evans B.W. (1977) - Antigorite-Ophicarbonates: Contact Metamorphism in Valmalenco, Italy. *Contribution to Mineralogy and Petrology*, 62, 301-312.

Tumiati S., Casartelli P., Mambretti A., Martin S., Frizzo P. and Rottoli M. (2005) - The ancient mine of Servette (Saint-Marcel, Val D'Aosta, Western Italian Alps): a mineralogical, metallurgical and charcoal analysis of furnace slags. *Archaeometry*, 47, 2, 317-340.

Whiteman J.A. and Okafor E.E. (2003) - Characterization of Nigerian bloomery iron smelting slags. *Historical Metallurgy*, 37, 2, 71-84.

Submitted, May 2014 - Accepted, October 2014